



HAL
open science

Progastrin production transitions from Bmi1⁺/Prox1⁺ to Lgr5^{high} cells during early intestinal tumorigenesis

Julie Giraud, M. Foroutan, Jihane Boubaker-Vitre, Fanny Grillet, Zeinab Homayed, U. Jadhav, Philippe Crespy, Cyril Breuker, J-F. Bourgaux, J. Hazerbroucq, et al.

► To cite this version:

Julie Giraud, M. Foroutan, Jihane Boubaker-Vitre, Fanny Grillet, Zeinab Homayed, et al.. Progastrin production transitions from Bmi1⁺/Prox1⁺ to Lgr5^{high} cells during early intestinal tumorigenesis. *Translational Oncology*, 2020, 14 (2), pp.101001. 10.1016/j.tranon.2020.101001 . hal-03090781

HAL Id: hal-03090781

<https://hal.science/hal-03090781>

Submitted on 12 Jan 2021

HAL is a multi-disciplinary open access archive for the deposit and dissemination of scientific research documents, whether they are published or not. The documents may come from teaching and research institutions in France or abroad, or from public or private research centers.

L'archive ouverte pluridisciplinaire **HAL**, est destinée au dépôt et à la diffusion de documents scientifiques de niveau recherche, publiés ou non, émanant des établissements d'enseignement et de recherche français ou étrangers, des laboratoires publics ou privés.



Distributed under a Creative Commons Attribution - NonCommercial - NoDerivatives 4.0 International License



ELSEVIER

Contents lists available at ScienceDirect

Translational Oncology

journal homepage: www.elsevier.com/locate/tranon

Original Research

Progastrin production transitions from $Bmi1^+/Prox1^+$ to $Lgr5^{high}$ cells during early intestinal tumorigenesis

J. Giraud^a, M. Foroutan^{b,c,1}, J. Boubaker-Vitre^{a,1}, F. Grillet^a, Z. Homayed^a, U. Jadhav^d, P. Crespy^a, C. Breuker^a, J-F. Bourgaux^e, J. Hazerbroucq^f, C. Pignodel^f, B. Brulin^a, R.A. Shivdasani^d, P. Jay^a, F. Hollande^{b,c,2}, J. Pannequin^{a,2,*}

^a IGF, Univ. Montpellier, CNRS, INSERM, Montpellier, France

^b Department of Clinical Pathology, The University of Melbourne, Victorian Comprehensive Cancer Centre, Melbourne, VIC 3000, Australia

^c University of Melbourne Centre for Cancer Research, Melbourne, VIC 3000, Australia

^d Dana-Farber Cancer Institute and Harvard Medical School, Boston, MA, USA

^e Service d'Hépatogastroentérologie, CHU Carémieu, Nîmes, France

^f Service d'Anatomo-Pathologie, CHU Carémieu, Nîmes, France

ARTICLE INFO

Keywords:

Lgr5 (GPR49)
Progastrin
Intestinal stem cells
Adenomas
Tumor initiating cells

ABSTRACT

Progastrin is an unprocessed soluble peptide precursor with a well-described tumor-promoting role in colorectal cancer. It is expressed at small levels in the healthy intestinal mucosa, and its expression is enhanced at early stages of intestinal tumor development, with high levels of this peptide in hyperplastic intestinal polyps being associated with poor neoplasm-free survival in patients. Yet, the precise type of progastrin-producing cells in the healthy intestinal mucosa and in early adenomas remains unclear. Here, we used a combination of immunostaining, RNAscope labelling and retrospective analysis of single cell RNAseq results to demonstrate that progastrin is produced within intestinal crypts by a subset of $Bmi1^+/Prox1^+/LGR5^{low}$ endocrine cells, previously shown to act as replacement stem cells in case of mucosal injury. In contrast, our findings indicate that intestinal stem cells, specified by expression of the Wnt signaling target LGR5, become the main source of progastrin production in early mouse and human intestinal adenomas. Collectively our results suggest that the previously identified feed-forward mechanisms between progastrin and Wnt signaling is a hallmark of early neoplastic transformation in mouse and human colonic adenomas.

Introduction

The tumor-promoting peptide progastrin (PG), encoded by the *GAST* gene (GeneID: 14459) [1,2,3], is a target of the WNT/ β -catenin pathway [4], a main driver of early colon tumorigenesis [5]. In addition, *GAST* is a target of the K-RAS pathway, activated in 50% of colorectal tumors [6]. This transcriptional regulation, coupled with the inability of colonic cells to fully process progastrin into shorter amidated forms as seen in the gastric antrum [7], likely explain why progastrin is abnormally secreted by 80% of tumors from patients with colorectal cancer [8,9].

This abnormal secretion of PG could be of paramount importance because it could be detected as early as the adenoma formation step in human [10] and could help to distinguish a subtype of human hyper-

plastic polyps that possess malignant potential [11]. Overexpression of a human version of PG into the blood of mice resulted in an increase of colonic crypt size [12]. In the same animal model, colonic epithelium mitotic cell number enhanced in physiological conditions as well as in response to DNA damage [13,14]. Thus, PG secretion seems to be very important in case of stress and is considered as a co-carcinogenic factor [15,16,17].

Because *Gast* KO mice are viable, Progastrin is known not to be indispensable for intestinal homeostasis [18]. Nevertheless, Do and colleagues showed that PG protein production is observed in approximately 2.6% of normal human colonic cells from resected non-diverticulum and, interestingly, it is more highly expressed in normal mucosa adjacent to hyperplastic polyps with malignant potential [11]. Similarly, Smith reported that about 5% of normal colonic cells produce PG and this amount of PG producing cells increased up to 40% in adenomatous

Abbreviations: APC, Adenomatous Polyposis Coli; DAPI, 4',6-diamidino-2-phenylindole; FACS, Fluorescence-Activated Cell Sorting; EGFP, Enhanced Green Fluorescence Protein; SPF, Specific Pathogen Free; Lgr5, leucine-rich repeat containing G protein-coupled receptor 5; PG, progastrin; CBC, crypt base columnar cells.

* Corresponding authors.

E-mail addresses: frederic.hollande@unimelb.edu.au (F. Hollande), julie.pannequin@igf.cnrs.fr (J. Pannequin).

¹ These authors equally contributed to this work.

² These authors jointly supervised this work.

<https://doi.org/10.1016/j.tranon.2020.101001>

Received 31 July 2020; Received in revised form 30 November 2020; Accepted 15 December 2020

1936-5233/© 2020 Published by Elsevier Inc. This is an open access article under the CC BY-NC-ND license (<http://creativecommons.org/licenses/by-nc-nd/4.0/>)

polyp lesions [10]. Furthermore, Jin et al demonstrated that intestine of PG-overexpressing mice contain more Lgr5-expressing stem cells than wild type animals [19]. Finally, we have recently published that PG is preferentially produced by cancer stem-like cells in adenocarcinomas [20]. Collectively these data strongly suggest that PG is produced at a low level in the healthy intestine and that it may contribute with other factors to maintain tissue homeostasis. It also indicates that progastrin secretion increases during early steps of tumorigenesis and that this secreted factor contributes to the niche of tumor-initiating cells.

Yet, the exact nature of progastrin-producing cells in the healthy intestine and during early adenoma formation remains unresolved. To address this question, we used immunostaining, RT-qPCR, single-cell RNAseq data analysis, and in situ RNAscope detection on murine and human healthy or preneoplastic intestinal tissues to perform a detailed quantitative and qualitative analysis of PG producing cells under physiological conditions, after radiation-induced stress and during early stage tumorigenesis. We show that PG is produced by a subset of Bmi1+/Prox1+ enteroendocrine cells in the healthy intestine but becomes predominantly produced by LGR5-high tumor-initiating cells in mouse and human adenomas. Our results demonstrate that PG production in Lgr5- high cells represents a signature event of the early activation of Wnt signaling during the first step of intestinal tumorigenesis.

Materials and methods

Human tissue collection

All human tissues were collected from the Nimes University Hospital under Human ethics agreement NCT#2011-A01141-40. 5 human intestinal adenoma (adenomatous and hyperplastic) sections and 5 non-inflamed human intestinal sections were collected from patients with diverticulitis. Informed consent was obtained from all patients. Protocols have been approved by AFASAAPS and ANSM.

Mice

The *Apc^{fl/fl} / Lgr5-EGFP-IRES-Cre^{ERT2}* strain was obtained by matting *Apc^{fl/fl}* mice (kindly provided by Christine Perret, Institut cochin, [21]) with *Lgr5-EGFP-IRES-Cre^{ERT2}* [22] animals (purchased from Jackson laboratories). Genotyping has been performed according to protocols and primer sequences provided in the associated publications [21,22]. Double inactivation of *Apc* in the Lgr5- high intestinal stem cells was induced by a single intra-peritoneal injection of 2 mg tamoxifen (Sigma). Wild-type animals used in this study had a C57BL/6 genetic background. Mice were maintained in SPF animal facilities (IGH) and were sacrificed for studies between 6 and 16 weeks old. All protocols for animal used were approved by the French guidelines recommendation (ethical committee no. 36). Sequences of primers used for genotyping *Apc^{fl/fl}* and *Lgr5-EGFP-IRES-Cre^{ERT2}* mice are referred in respective paper [21,22].

Immunostaining/microscopy

For tissue preparation, small intestine and colon were dissected from adult mice and fecal contents were flushed out with PBS. After fixation with 4% paraformaldehyde for 4 hours at room temperature, small intestine and colon were rolled up using the "swissroll" technique, dehydrated, embedded in paraffin and sectioned into 5 μ m slices.

For immunofluorescence staining, sections were first dewaxed by heating them at 56 °C and immersing them in serial xylene and ethanol baths. Antigens were unmasked in boiling citrate buffer pH 6 for 20 min and non-specific sites were blocked for 1 h in blocking buffer (PBS containing 5% milk and 0,5% triton). Slides were then incubated overnight at 4 °C with primary antibodies diluted in blocking buffer. After washing, samples were incubated 1 h at room temperature with fluorescent secondary antibodies (FluoroProbe, Alexa488 or Alexa594), nuclei were stained with DAPI (FluoroProbe) and finally samples were mounted in

fluoromount G (SouthernBiotech). Slides were observed using an epifluorescent microscope (Zeiss AxioImager Z1 apotome).

For immunohistochemistry staining, endogenous peroxidase activity was quenched with H₂O₂/methanol 1:20 for 20 min at room temperature. Secondary antibodies were coupled to peroxidase (Histofine) and staining was developed with Fast DAB (brown precipitate, Sigma Aldrich) and hematoxylin counterstain was used. After dehydration, sections were mounted in Pertex (Histolab). Slides were scanned using NanoZoomer 2.0 HT ® (Hamamatsu) and analyzed with NDP View (Hamamatsu) software.

Dissociation of intestinal epithelium

Small intestine and colon were dissected from adult mice (10–16 weeks old for crypt/villi experiment, 14–16 for tamoxifen experiments) and fecal contents were flushed out with cold PBS. Part of small intestine and colon were reversed and were first incubated in 10 mM DTT/HBSS for 10 min on ice to remove mucus. Then, tissues were incubated in 10 mM EDTA/HBSS (without Calcium and without Magnesium) for 15 minutes on ice and villi were mechanically detached after vibration of the tissue reversed in 0.1%BSA/PBS solution for 5 min. This step was repeated again twice and then crypts were harvested following other 2–3 series of vibrations in 0.1%BSA/PBS solution. Purity of each fraction was validated under microscope and villi or crypts were pelleted at 250 g for 5 min. Total RNA was extracted with trizol reagent (Ambion), DNA was removed using DNaseI treatment, and RNA was then purified on microRNAeasy column (Qiagen). In parallel, total RNA was extracted from whole undissociated samples of the jejunum and colon.

Flow cytometry

For Fluorescence-Associated Cell Sorting experiments, villi or crypt fractions were dissociated for 20 min at 37 °C under gentle agitation in HBSS solution containing dispase (0.25 U/mL, Stem cell technology), DNase I (10 U/mL, Sigma Aldrich) and FCS 2%. Cells were then passed through a 70- μ m filter and alive cells were counted using trypan blue. Dissociated cells were stained for 30 min on ice with Anti-EpCAM antibody coupled to APC fluorochrome (eBioscience 17-5791, 1 μ l/10⁶ cells) diluted in Advanced DMEM-F12 (Gibco) medium. Finally, after washing with medium, dissociated cell were maintained on ice in fresh Advanced DMEM-F12 containing 10 μ M of ROCK kinase inhibitor Y27632 (Sigma) until FACS purification. Cells were sorted using FACSAria™ II (BD Biosciences) or MoFlo®Astrios™ (Beckman Coulter, Inc) and BD FACSDiva™ Software (BD Biosciences) or Summit 6.0™ Software (Beckman Coulter, Inc) were used to analyze signal. Dead cells were excluded based on light scatter characteristics and 7-Amino-actinomycin D (7-AAD, Invitrogen) exclusion. Epithelial cells were EpCAM-positive (APC channel) and LGR5- high stem cells were EGFP-positive (FITC channel).

RNA in situ hybridization (RNAscope)

Progastrin and LGR5 mRNA expression were detected using the RNAscope assay (Advanced Cell Diagnostics, Hayward, CA) according to the manufacturer protocols. Briefly, FFPE human polyps sections were dewaxed, incubated 10 min at 40 °C with H₂O₂, boiled 15 min at 100 °C for target retrieval then treated 15 min at 40 °C with Protease Plus. The tissues were hybridized with Gast probe (Cat. No. 311071) and Lgr5 probe (Cat. No. 311021) at 40 °C in a HybEZ oven for 2hrs before incubation with AMP-1 to -3 reagents following by development of HRP signals (Lgr5 probe, fluorescein; Gast probe, cyanine 3) and DAPI counterstains. The signals were visualized using the Multiplex Fluorescent assay v2. Tissue quality and mRNA integrity were validated using the 3-plex Negative control Probe (Cat. No. 320817) and 3-plex Positive control Probe (Cat. No. 320861).

Retrospective RNAseq data analysis

Expression of *Gast* and other genes was analyzed in bulk RNAseq data generated from several mouse intestinal cell types as published by Jadhav et al [23]. The gene count data was downloaded on 14/09/2018 from the Gene Expression Omnibus (GEO ID: GSE83394). Genes were filtered to only keep those with count-per-million (CPM) > 1 in at least one sample and log(CPM) values were calculated using the edgeR (v. 3.26.7) R/Bioconductor package [24].

We also retrospectively analyzed single cell RNAseq data generated from several flow cytometry purified mouse intestinal cell populations reported by Yan et al [25]. Yan et al released the data for 4 samples generated in parallel, each with 2 technical replicates. These include *Bmi1+*, *Prox1+*, *Lgr5-high* and *Lgr5-low* samples, generating 4500 single cells. The data were downloaded on the 14/09/2018 from GEO ID: GSE99457. We read the data into R (v. 3.6.0) using the read10X function from the edgeR (v. 3.26.7) R/Bioconductor package, and stored as SingleCellExperiment object using the SingleCellExperiment R/Bioconductor package (1.6.0)

The NCBI RefSeq annotation data were used to convert gene aliases to official gene symbols. We filtered out genes that were expressed in fewer than 1% of the total cells, and those with no valid official symbols, as well as duplicated genes. We also removed cells with more than 20% mitochondrial UMI counts which resulted in 3558 cells.

We used the *scran* (v. 1.12.1) R/Bioconductor package [26] to normalize the gene counts, calculated natural log of the normalized data, and then converted this to a Seurat object using the Seurat (v. 3.0.2) R package [27,28,29] to find 2000 most variable genes and perform principle component analysis (PCA). Using the first 20 principal components (PCs) and the Seurat package, we then performed t-distributed stochastic neighbor (t-SNE – through the *Rtsne* [v. 0.15] R package) as well as uniform manifold approximation and projection embedding (UMAP - through *umap-learn* Python package installed using the *reticulate* [v. 1.13] R package).

Finally, we converted Seurat object to SingleCellExperiment and performed clustering by running model-based clustering from *mclust* (v. 5.4.5) R package [30] on the first two PCs, which resulted in 9 clusters. These clusters were then used with *slingshot* (v. 1.2.0) R/Bioconductor package to infer lineage structure and generate smooth lineage curves. We used *ggplot2* (v. 3.2.1), *ggpubr* (v. 0.2.2) and *RcolorBrewer* (v. 1.1-2) R packages for data visualisations, as well as *dplyr* (v. 0.8.3) and *tidyr* (v. 0.8.3) for data manipulation.

The R Markdown for these analyses can be provided upon request

Real-time PCR. RNA extraction and real-time PCR

Total RNA was extracted using the RNeasy mini kit (Qiagen) and treated with DNase-1 according to manufacturer recommendations. Total RNA was quantified using nanodrop, 200 ng was reverse transcript using SuperScript II reverse transcriptase (Invitrogen) and oligo dT primers according to manufacturer. Relative gene expression was measured in duplicate by real-time PCR using SYBR Green I Kit (Roche Diagnostics) and LightCycler480 instrument (Roche). Results were normalized with GAPDH expression following house keeping gene test amongst 8 of them. We runned in parallel no template control and assessed the absence of DNA contamination using a no RT assay when first extracting RNA. The fold changes in genes expression were calculated with the 2- $\Delta\Delta C_t$ method.

Primer sequences used are as follow:

Mouse primers: *mCrypdin 5* (defensin alpha 5, *Defa5*, GeneID: 13239) forward (5'-AGGCTGATCCTATCCACAAAACAG-3') and reverse (5'-TGAAGAGCAGACCTTCTTGGC-3'); *Gapdh* (GeneID: 14433) forward (5'-TGCAAGTGGAGATTGTTGC-3') and reverse (5'-AAGATGGTGTGGCTTCCCG-3'); *Lgr5* (GeneID: 14160) forward (5'-GAGCGGGACCTTGAAGATTTCCT-3') and reverse (5'-GCCAGCTACCAATAGGTGCTCA-3'); *Gast* (GeneID: 14459)

forward (5'-AACAGCCAACCTATTCCCCAG-3') and reverse (5'-CCAGCTAAGACCAGCATG-3'); *Tcf4* (GeneID: 21413) forward (5'-TCTAGCAATAATCCCGCAGCGCGCTCTTCA CAGTAGT -3') and reverse (5'-ACTACTGTGAAGAGGCGCCGCTGCGGGATTATTGCTAGA -3'); *Fabp* (GeneID: 14077) forward (5'-CAGAAGTGGGATGGAAAGTCCG -3') and reverse (5'-CGACTGACTATTGTAGTGTTTGA-3'); *EGFP* forward (5'-GAGCTGAAGGGCATCGACTTCAAG-3') and reverse (5'-GGACTGGGTGCTCAGGTAGTGG-3').

Statistical analysis

For each experiment, data are presented as the mean of a minimum of 3 independent experiments +/- SEM. All statistical tests were 2-sided and a 5% cutoff was used to validate result significance (* $P < .05$, ** $P < .01$, *** $P < .001$, **** $P < .0001$) and were performed using the GraphPad Prism Version 6 software. Tests performed were either Mann-Whitney, Student t-test or Kruskal-Wallis indicated in figures legends.

Results

Progastrin is produced by cells located in the lower section of mouse intestinal and colonic crypts

To identify progastrin in the mouse intestinal and colonic mucosa we first used immunohistochemistry and immunofluorescence detection with an antibody raised specifically against this peptide [20]. We found that this peptide was produced by rare cells located in the lower part of the crypt in the small intestine (Fig. 1A and B) and in the colon (Fig. 1C and D) of wild type C57BL/6 mice. This staining was specific for Progastrin since it was quenched by pre-incubation of the antibody with recombinant Progastrin, and the secondary antibody displayed no significant background (supplementary Fig. S1). To quantify progastrin expression in the small intestine and colon of wild type mice, we used quantitative RT-PCR on RNA samples extracted after epithelium dissociation and small intestinal crypt and villi separation in wild-type mice (Fig. 2). Enrichment of crypt vs villi epithelial fractions was verified qualitatively using imaging (Fig. 2A), as well as quantitatively using primers that amplify crypt-specific genes, namely *Defa5* and *Lgr5* (Fig. 2B). Expression of the *Gast* mRNA, which encodes progastrin, was enriched by 73-fold in the epithelial crypt compartment in comparison with the villi (Fig. 2B). We then used laser-capture microdissection to separate the lower and upper sections of wild type mice colonic crypts (supplementary Fig. S2A). Enrichment of lower and upper sections was validated through the quantification of differential expression for *Tcf4* and *Fabp* genes, respectively, and we found that the expression of *Gast* was strongly enriched in the bottom section of colonic crypts (supplementary Fig. S2B).

The mouse Lgr5-high stem cell is not the progastrin producing cells in healthy intestinal tissue

Our results indicate that progastrin is expressed in the lower section of intestinal and colonic crypts in wild-type mice, an area known to contain the intestinal stem cells. Because we recently showed that PG was preferentially expressed by cancer-stem like cells in comparison with differentiated cells in the context of colorectal carcinomas [20], we asked whether normal intestinal stem cells were expressing PG encoding gene in wild type mice. To address this question we used mice harboring a *Lgr5-EGFP-IRES-creERT2* "knock-in" allele that drives *Lgr5* haploinsufficiency and enables the expression of EGFP and CreERT2 fusion protein from the *Lgr5* promoter/enhancer elements [22]. In the small intestine and colon, EGFP fluorescence is thus restricted to *Lgr5*-high crypt base columnar cells, which are widely recognized as intestinal stem cells [22]. To determine whether *Lgr5*-high cells produce progastrin, we purified EGFP/EpCAM double-positive, ie *Lgr5*-expressing intestinal epithelial cells, using fluorescence-associated cell sorting after enzymatic dissociation of the small intestinal and colonic mucosa.

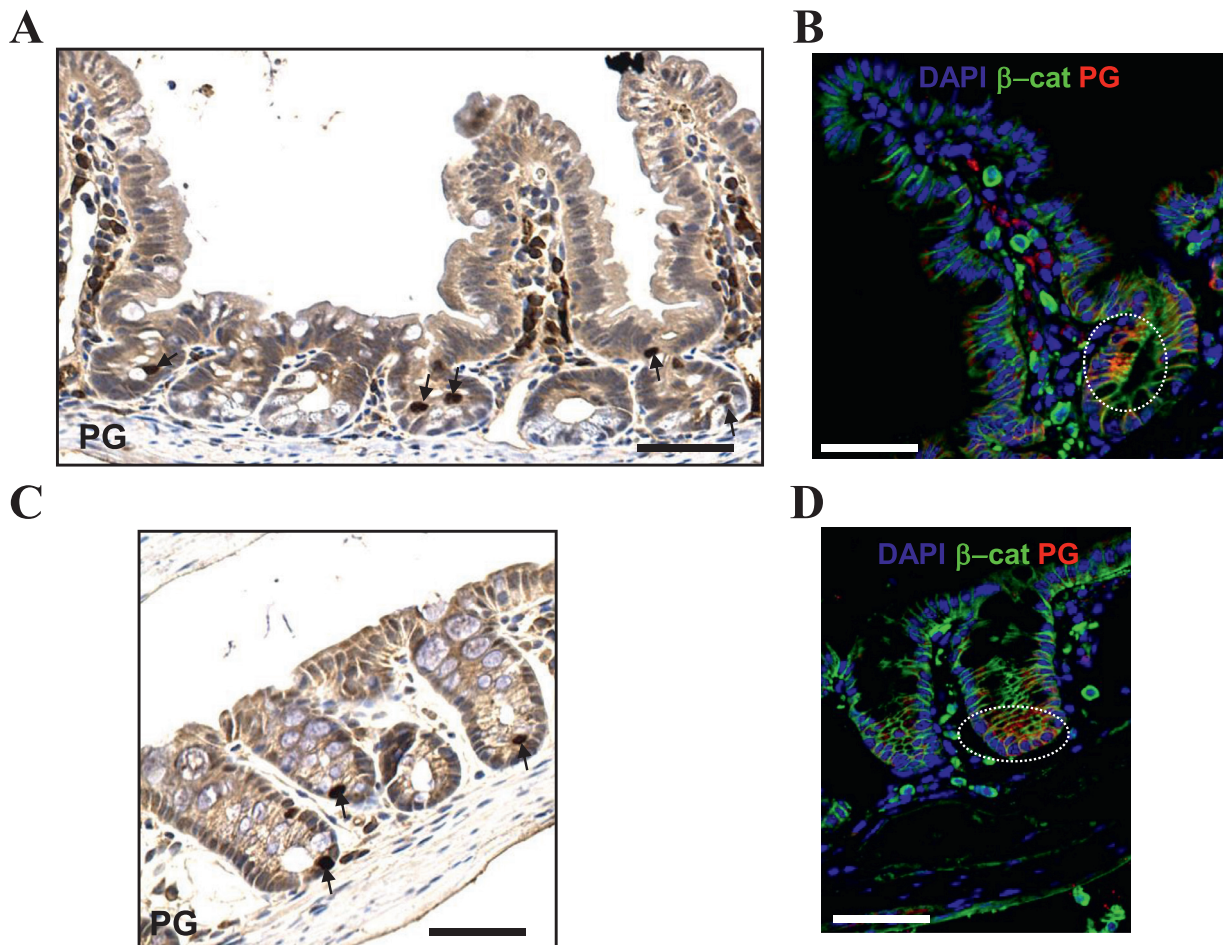


Fig. 1. Progastrin expression in the mouse intestinal and colonic epithelium. Progastrin is expressed in a small number of cells localized in the mouse small intestine crypt (A, B) and colon (C, D). (A, C) Immunohistochemical detection of progastrin (PG)-expressing cells in mouse intestinal sections. Nuclei are counterstained with hematoxylin. Arrows point to progastrin-positive cells. (B, D) Immunofluorescent detection of progastrin (PG) (Alexa 594, red) and β -catenin (β cat, A488, green) in mouse intestinal sections. Nuclei are stained with DAPI (blue). Dotted lines highlight areas of progastrin-positive cells. Scale bars, 50 μ m. (For interpretation of the references to color in this figure legend, the reader is referred to the web version of this article.)

Wild type C57BL/6 mice were used as negative controls in this experiment. FACS profiles showed that EGFP-positive cells represent 2.6% and 10.7% of live epithelial cells (EpCAM+) isolated from the crypt of small intestine and colon (Fig. 3A and B respectively). RNA was extracted from purified EpCAM+/EGFP+ and EpCAM+/EGFP- cells, and quantitative RT-PCR was performed to compare the expression of *Gast*, *Lgr5* and *EGFP* mRNAs in these populations. As expected EGFP mRNA was strongly enriched in EpCAM+/EGFP+ cells. The *Lgr5* mRNA was also enriched strongly significantly, albeit to a lesser degree. In contrast, *Gast* gene expression was mostly detected in EGFP-negative cells but was much lower or not detectable in EGFP-positive crypt base columnar cells (CBCs) of the small intestine and colon (Fig. 3C and D).

Taken together these results demonstrate that PG is preferentially produced by cells located in the lower part of intestinal crypts but that these cells are not the LGR5-high intestinal stem cells.

Progastrin is expressed by Bmi1-positive/Prox1-positive endocrine cells in the intestinal crypts

Progastrin was originally identified as the unmaturing precursor for the digestive hormone amidated gastrin in the gastric mucosa, where it is secreted by G cells in the gastric antrum [31]. In the intestinal mucosa, the presence of cells expressing progastrin was first suggested by Finley et al., in 1993 [32], who suggested that some of these cells may also express the enteroendocrine marker Chromogranin A. In the

present study, while progastrin-positive immunostaining was sometimes detected in cells that also expressed chromogranin A, a significant number of cells were found to only express one of these two genes. Indeed, chromogranin A was not detectable in all progastrin-expressing cells, and all chromogranin A positive cells did not express progastrin (Supplementary Fig. 3A), suggesting that these two cell populations do not completely overlap.

To gain further insight into the epithelial cell subpopulation that expresses progastrin in the intestine, we analyzed whether progastrin RNA expression could be detected in previously published RNAseq data from intestinal cell subpopulation [23]. *Gast* mRNA expression was low but readily detectable in cells expressing a GFP knock-in under the control of the *Bmi1* promoter (Supplemental Fig. S3B), and this result was confirmed using RT-qPCR in purified *Bmi1*^{GFP} cells from the same animals (Supplemental Fig. S3C). Since *Bmi1*^{GFP} cells were previously shown to transition towards a *Lgr5* intestinal stem cell phenotype following 10 Gy whole-body irradiation [23], we also determined whether progastrin remained expressed in these cells as they progressively lose their *Bmi1*-positive cell characteristics to acquire *Lgr5*-high cell features. Interestingly we found that *Gast* expression in transitioning *Bmi1*^{GFP} cells was drastically reduced 24 h and 36 h after irradiation of the intestinal mucosa (Supplementary Fig. S3C), although previous reports indicated that progastrin production in the intestine does not disappear after irradiation and that this peptide plays a significant role in radioresistance [33]. Together these results indicate that progastrin expression is a fea-

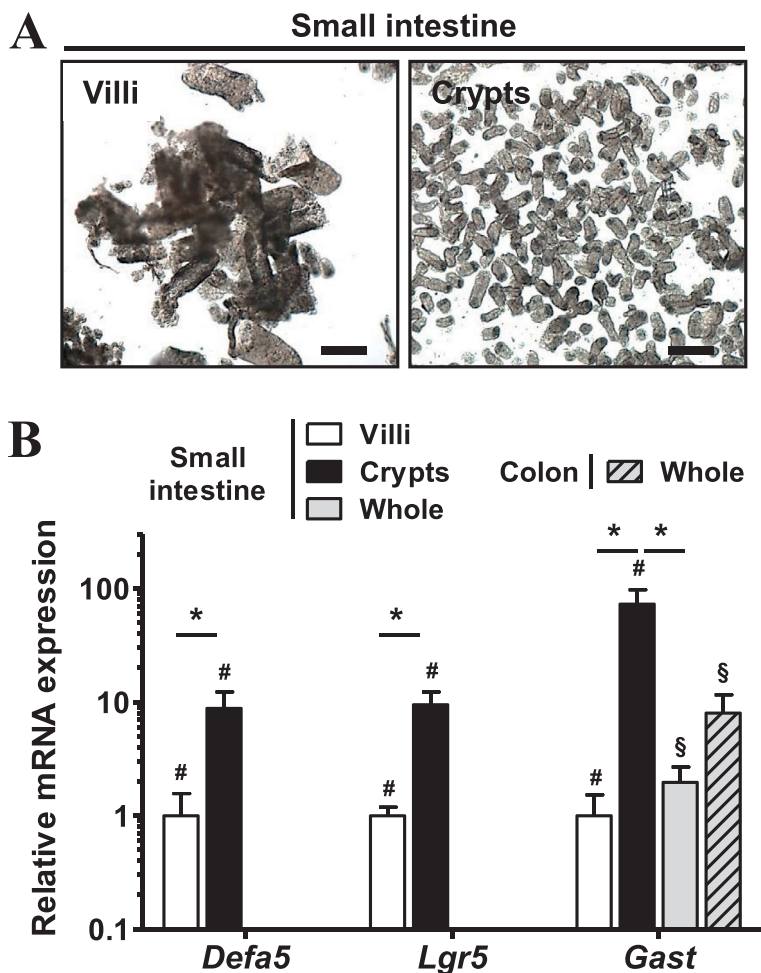


Fig. 2. Progastrin is produced by cells localized in the crypt proliferative compartment within the mouse healthy intestine. (A) Representative phase-contrast image of villi (left) or crypts (right) harvested after the dissociation of the mouse small intestine. Scale bar, 50 μ m. (B) Relative expression of *Defa5*, *Gast* and *Lgr5* mRNA in mice small intestine (villi: white bars; crypts: black bars; whole: grey bar) or colon (whole: striped grey bar) measured by qRT-PCR. * $P < 0, 05$ Mann – Whitney (*Defa5* and *Lgr5*) or Kruskal-Wallis tests (*Gast*). Data are presented as the mean with SEM, $n = 7$ (#) or 4 mice (§).

ture of at least some *Bmi1*-positive cells in the healthy intestinal mucosa, and suggest that production of this peptide decreases in these cells during the early stage of their phenotypic transition into *Lgr5*-positive intestinal stem cells following irradiation.

Although *Bmi1* expression was originally thought to be a defining feature of the “+4” cancer stem cells originally identified by Potten [34], recent studies have provided definitive evidence that it is expressed in all proliferative cells within the crypt, including in *Lgr5*-high cells [35,36]. To refine our understanding of which intestinal epithelium cell types express progastrin, we analyzed previously published single cell RNA sequencing (scRNAseq) datasets generated in mouse intestinal cells. Since the expression levels for this gene are known to be low in the normal intestinal tissue, we first set out to determine whether *Gast* expression could be reliably detected in scRNAseq datasets. We were not able to use *Gast* expression data in some of these datasets, either due to the raw data filtering approach [37] or to the *Gast* gene not being annotated [38]. However *Gast* expression was reliably detected in recent scRNAseq data generated by the Cuo lab [25]. Expression of *Gast* was restricted to the *Bmi1*+/*Prox1*+ population defined by Yan et al as a reserve stem cell population (Fig. 4A and B). Beyond expressing *Bmi1* and *Prox1*, *Gast*+ cells were also found to express high levels of *Scg2* (chromogranin C), intermediate levels of chromogranin B, and low to undetectable levels of chromogranin A (Fig. 4C). *Lgr5* was virtually not expressed in these cells, corroborating our earlier RT-qPCR results (Fig. 3). Paneth cells markers (*Defa5*, *Lyz1*) clearly delineated a different, *Gast*-negative population (Fig. 4C). In addition, we also analyzed the expression of *Uri1*, which encodes the unconventional prefoldin RBP5 interactor and was recently described by Chaves-Pérez et al. as labelling an intestinal cells subset that promotes tissue generation after irradiation. Low level ex-

pression of *Uri1* was detected in a majority of cells, including the populations defined as *Lgr5*-high and *Bmi1*-positive by Yan et al., including *Gast*-expressing cells. However, the highest *Uri1* expression was detected in two subsets of *Gast*-negative/*Bmi1*-positive cells, one of which also expressed *Prox1* while the other was *Prox1*-negative but strongly positive for *Chrga* and *Chrgb* expression (Fig. 4C). Altogether, our finding suggests that *Gast*+ cells represent a subset of the *Bmi1*+/*Prox1*+ population of injury-inducible reserve intestinal stem cells identified by Yan et al [25] and Jadhav et al [23].

In addition, to gain further insight into putative progastrin target cell populations in the healthy intestinal mucosa, we also quantified the expression of putative progastrin receptors in the same dataset (Fig. 4D). As expected *Annexin-II* (*Anxa2*), one of these candidate receptors [39], was ubiquitously expressed in most intestinal epithelial cells. In contrast, the recently identified progastrin receptor GPR56 [40], a member of the adhesion GPCR family encoded by the *Adgrg1* gene, had a more restricted expression pattern. Indeed, *Adgrg1* was expressed in a subset of *Bmi1*+/*Prox1*+ cells, in *Bmi1*+/*Prox1*^{neg} and in a subset of *Lgr5*-high cells (Fig. 4D), suggesting that progastrin may have both autocrine and paracrine roles in the healthy intestine. mRNAs for CCK2R, another suggested receptor for progastrin [40], were not detected in this dataset.

Tumor initiating cells produce progastrin in early mouse intestinal adenomas

Beyond its possible role in the healthy intestinal mucosa, multiple studies have demonstrated that progastrin overexpression promotes adenoma development, proliferation and increases *Lgr5*-high cell numbers in mice [19,4,2] and is associated with increased risk of neoplasia in humans [11]. In view of the instrumental role played by *Lgr5*-high cells

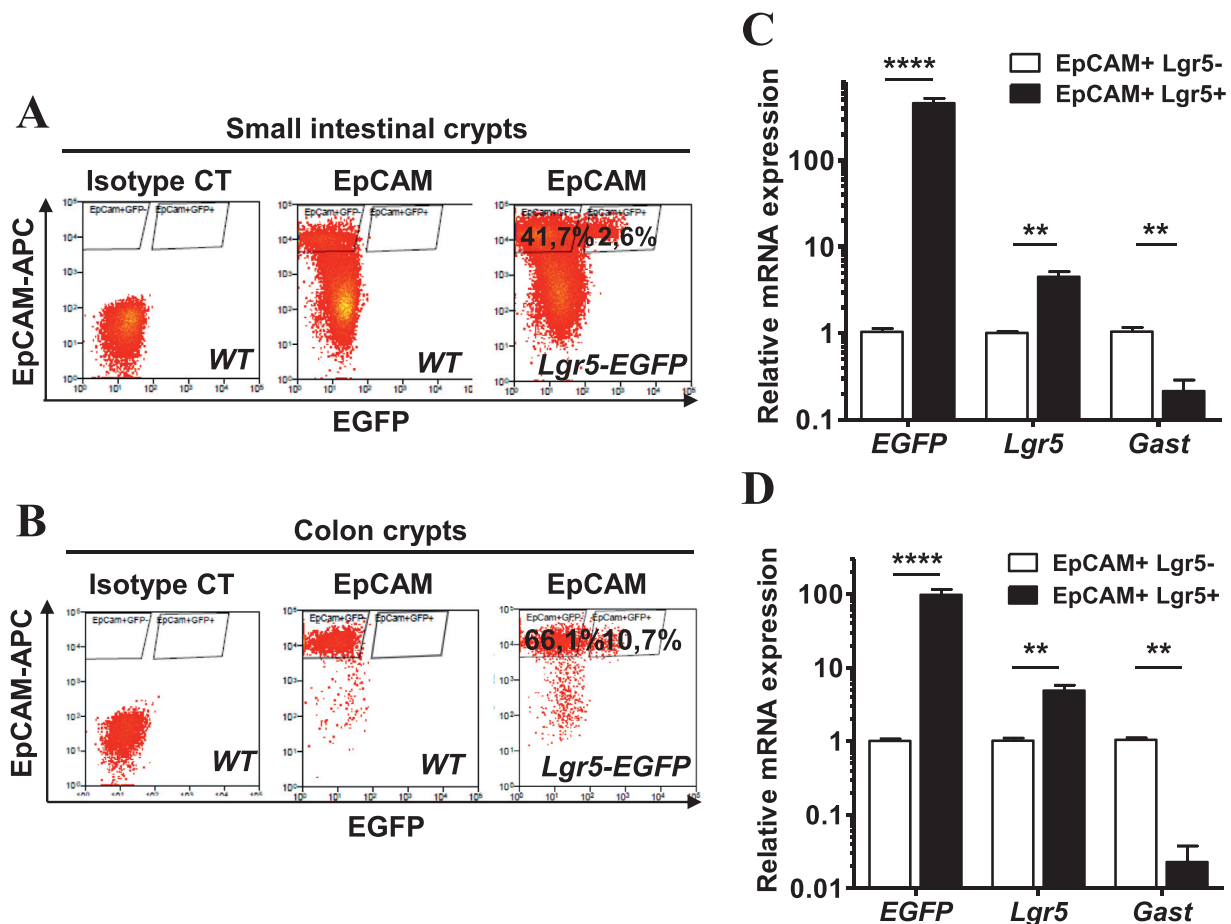


Fig. 3. Mice *Lgr5*-high intestinal stem cells are not the progastrin-producing cells. (A-B) Representative dot plots for flow cytometry-based EpCAM-APC and EGFP detection on crypts from small intestine (A) or colon (B), harvested from WT (middle panels) or *Lgr5-EGFP-IRES-Cre^{ERT2}* C57BL/6 mice (right panel), in comparison with isotype IgG staining as negative controls (left panels). (C-D) Expression of *EGFP*, *Lgr5* and *Gast* mRNA in epithelial (EpCAM positive) cells from mice small intestinal (C) or colonic crypts (D). mRNAs were quantified using qRT-PCR. ** $P < 0,01$, **** $P < 0.0001$, Mann – Whitney test. Data represents the relative expression in EpCAM+/Lgr5- high cells (black bars), expressed as fold-ratio of the expression in EpCAM+/Lgr5-low cells (white bars). Results are presented as the mean with SEM from $n = 3$ animals.

in early tumorigenesis in the mouse, we used a *Lgr5* cell-driven model of adenoma development to identify progastrin-producing cells during early stages of tumorigenesis.

To mimic the first step of tumorigenesis in mice, we crossed the *Lgr5-EGFP-IRES-creERT2* mouse with animals in which the 14th exon of the *Apc* gene was flanked by loxP sites [21]. Pups resulting from this crossing were genotyped and homozygous carriers were treated with a single dose of tamoxifen around 15 weeks of age to induce the depletion of both *Apc* alleles specifically in the *Lgr5*-high cells, which are detectable through their expression of EGFP. After a 2- or 4-week tamoxifen treatment, mice were euthanized and their intestinal adenomas were collected and processed for immunofluorescence staining experiments (Fig. 5A and B) or for flow cytometry-based separation of *Lgr5*-high vs *Lgr5*-low cells followed by RNA extraction and quantification (Fig. 5C). Using tissue sections from adenomas collected in these mice, we found that EGFP (surrogate for *Lgr5*-high cells) and progastrin immunostaining co-localized in small intestinal and colonic adenomas from these mice (Fig. 5A and B). In addition, RT-qPCR quantification confirmed the enrichment of *Lgr5* gene expression in EGFP-expressing cells and, in contrast with our earlier results in the healthy intestinal mucosa (see Fig. 3), *Gast* gene expression was enriched in the *Lgr5*-high cell fraction from adenomas (Fig. 5C) collected 2 weeks after tamoxifen induction. Collectively these results demonstrate that *Apc* invalidation acts as a switch to initiate progastrin pro-

duction preferentially in *Lgr5*-high tumor-initiating cells in the mouse intestine.

Human intestinal tumor initiating cells produce Progastrin

To validate our results on human samples we used the recently-developed highly sensitive RNAscope technique, which enables the amplification and fluorescence-based detection of mRNAs for genes of interest on FFPE tissue sections. This technique, which enables sensitive detection of low-expression targets, was carried out using probes against *LGR5* and *GAST* mRNA, enabling the quantification of cells that individually or jointly express these mRNA.

Negative and positive control probes were used to verify the applicability of this approach on FFPE patient adenoma tissue sections (Supplementary Fig. S4A). The specificity of the human *GAST* probe was validated on RKO colorectal cancer cells that were made to express high progastrin levels, in comparison with the low-expressing parental RKO line. As shown on Supplementary Fig. S4B the *GAST* RNAscope signal was clearly higher in RKO colon carcinoma cells made to overexpress Progastrin (right) than in control RKO cells (left). The *LGR5* probe was validated previously on similar tissues [41].

We then used these probes to detect progastrin- and *LGR5*-encoding mRNAs in macroscopically healthy human colonic crypts, as well as in early neoplastic lesions from the human colon. First, non-inflamed hu-

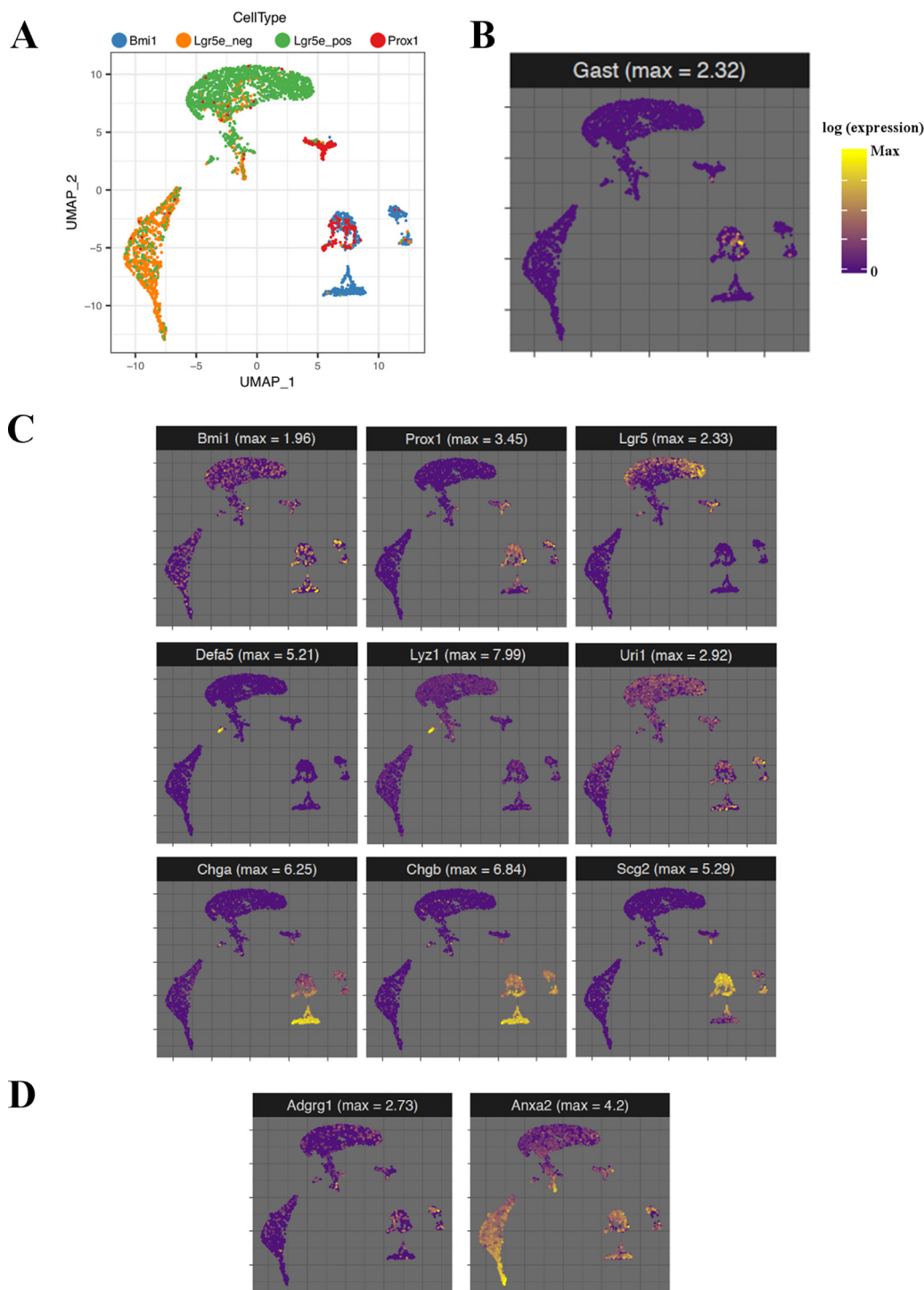


Fig. 4. Progastrin expression is restricted to Bmi1+/Prox1+ cells in the healthy intestinal epithelium. **(A)** UMAP plot representing the cell population subsets (Bmi1-positive, Lgr5-low, Lgr5-high, and Prox1-positive) described in the single cell RNAseq data by Yan et al [25]; **(B-D)** Expression pattern of multiple genes in the intestinal cell subsets depicted in A: **(B)** expression of *Gast*; **(C)** expression of cell fate markers *Bmi1*, *Prox1*, *Lgr5*, *Chga*, *Chgb*, and *Scg2* (chromogranin c); **(D)** expression of putative progastrin receptors *Adgrg1* and *Anxa2*. Expression levels are represented as the natural log of the normalized data, and the maximal expression level detected for each gene of interest is indicated above each panel.

man intestinal tissue collected from patients with diverticulitis were stained with the *GAST* and *LGR5* RNAscope probes (Fig. 6A). Intestine from patients with diverticulitis was chosen to represent healthy tissue since several studies have shown that inflammatory tumor microenvironment impact epithelial neighboring cells. In parallel, *GAST* and *LGR5* RNAs were also detected in FFPE tissue sections of intestinal adenomas from 5 patients with no prior family history of polyposis syndrome (Fig. 6B). Quantification of *GAST* and *LGR5* - high vs

low cells was then performed on multiple crypts per patient sample. Corroborating results obtained in mouse intestinal tissues (see Fig. 3) we found that, while progastrin expression is primarily a feature of LGR5-low intestinal cells in the healthy intestinal epithelium, a majority (>65%) of Progastrin-producing cells within adenomas are also LGR5-high (Fig. 6C). In accordance with this data and with results obtained in mouse tissues, we found that the overwhelming majority of LGR5-high cells (>80%) did not express detectable levels of progastrin in the

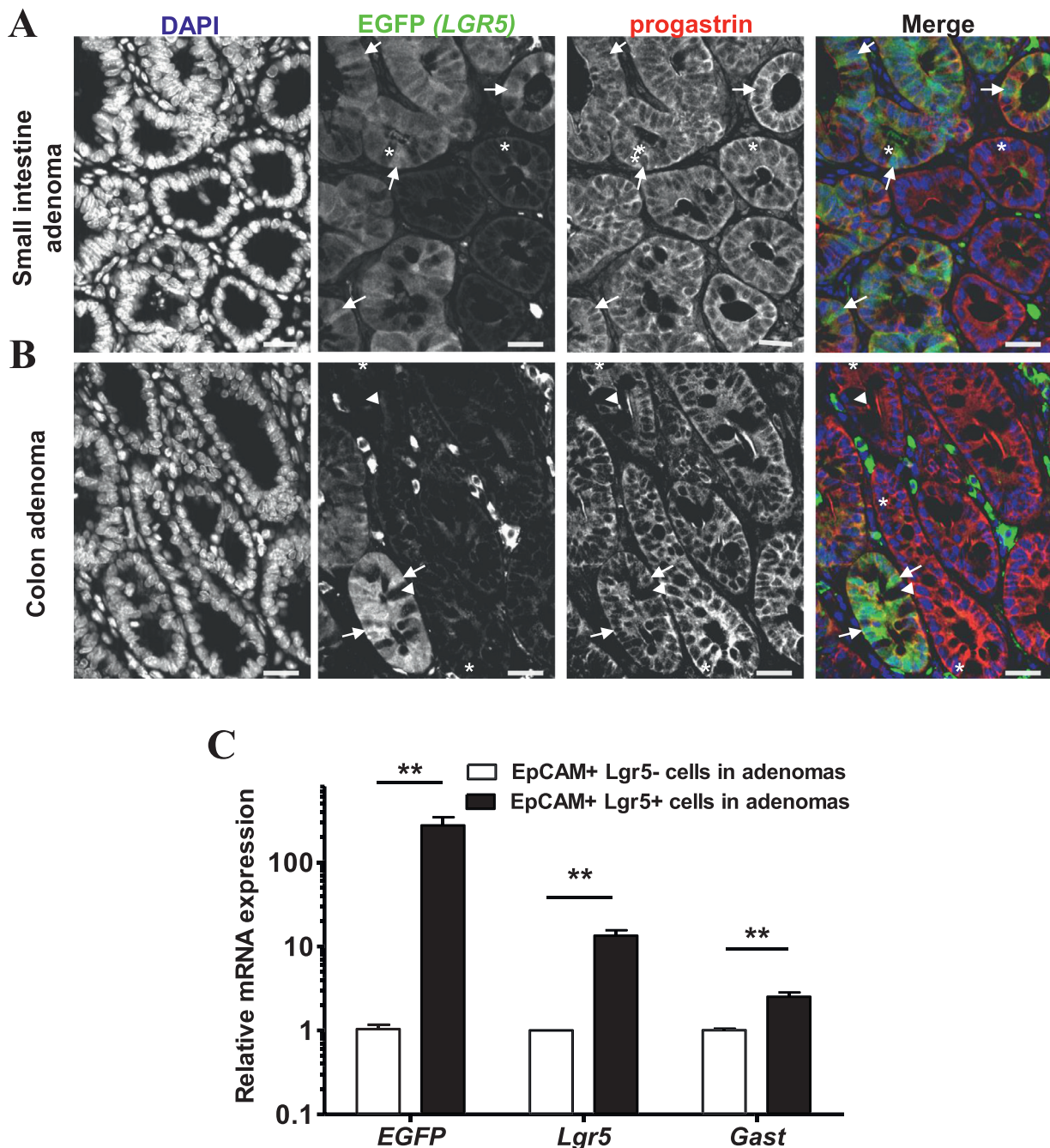


Fig. 5. Progastrin is expressed in Lgr5-EGFP+ adenoma stem cells in mice. **(A-B)** Immunofluorescence photomicrographs of small intestine **(A)** or colon **(B)** adenoma tissues from *Apc^{fl/fl} /Lgr5-EGFP-Cre^{ERT2}* mice treated with 2 mg tamoxifen 4 weeks before sacrifice. Arrowheads point to progastrin (Alexa 594, red)-positive cells within Lgr5-EGFP^{hi} cells (EGFP, Alexa 488, green), arrows mark Lgr5-EGFP^{hi} cells and arrowheads mark Lgr5-EGFP^{neg} cells. Note that all Lgr5-EGFP^{hi} cells express progastrin. Nuclei are counterstained with DAPI (blue). Scale bars, 25µm. **(C)** Relative mRNA expression of *EGFP*, *Lgr5* and *Gast* in intestinal adenomas (Lgr5 low: white bars; Lgr5- high: black bars) from *Apc^{fl/fl} /Lgr5-EGFP-Cre^{ERT2}* mice treated with 2 mg tamoxifen 2 weeks before sacrifice and measured by qRT-PCR. ** $P < 0,01$, **** $P < 0.0001$, Mann - Withney test. Data are presented as the mean with SEM, $n = 3$ animals. (For interpretation of the references to color in this figure legend, the reader is referred to the web version of this article.)

healthy colonic epithelium, but that most LGR5- high cells (90%) did express progastrin in colonic adenomas (Supplemental Fig. S5). A minority of LGR5- high cells also expressing PG was also observed in the so called normal epithelium distant from adenomas (data not shown).

Discussion

In the present work we sought to specify the nature of progastrin-producing cells in the healthy intestine and during early adenoma for-

mation, using several experimental and in silico approaches on murine and human healthy or preneoplastic intestinal tissue. Our results demonstrate that, in the healthy intestine, progastrin is produced by a subset of entero-endocrine cells previously shown to behave as a reserve stem cell population after epithelial injury. In contrast, progastrin expression is primarily a feature of Lgr5- high cells in preneoplastic intestinal lesions in the mouse as well as in human colonic adenomas.

Expression of progastrin in the healthy colonic mucosa was first suggested by Finley in 1993 [32]. While this original publication suggested

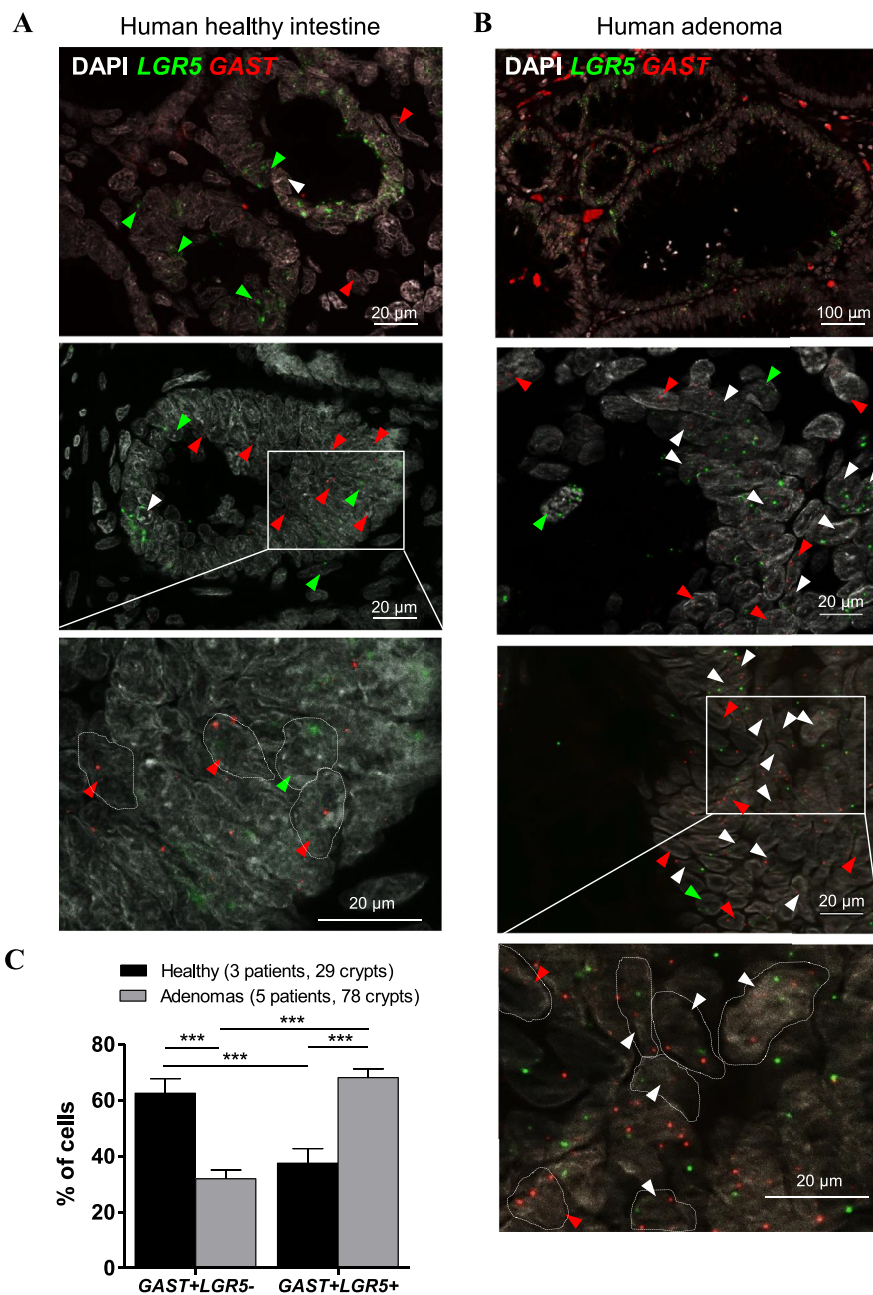


Fig. 6. Progastrin expression in the human colon transitions from LGR5-low to LGR5- high cells during early neoplasia. Tissue sections of macroscopically healthy human colonic mucosa from patients with diverticulitis (A) and of human colonic adenomas (B) were hybridized with RNAscope probes against *GAST* (red) and *LGR5* (green), and nuclei were counterstained with DAPI (white). Progastrin-positive cells are highlighted with red arrowheads, LGR5- high cells with green arrowheads, and double stained progastrin/LGR5- high cells with white arrowheads. Scale bars represent 100 or 20 μm as indicated on each panel. On high magnification images, white lines delimitate individual cells for better visualization of potential co-localization events (C) Bar graph representing the proportion of *LGR5*-low and *LGR5*- high cells among *GAST*-expressing cells, quantified in tissue sections from the healthy human colonic epithelium ($n = 3$ patients, black bars) and from colonic adenomas ($n = 5$ patients, grey bars). $p < 0.001$, Kruskal Willis test. (For interpretation of the references to color in this figure legend, the reader is referred to the web version of this article.)

that progastrin-secreting cells were co-expressing chromogranin A, our single cell RNaseq analysis suggests that these cells rather express high levels of *Scg2* (Chromogranin C) and to a lesser degree *Chgb* (Chromogranin B), and that some but not all also express Chromogranin A. Although the *GAST* gene is a target of the Wnt pathway [4], we did not detect significant progastrin expression in *Lgr5*- high cells within the healthy mouse epithelium. We instead detected progastrin expression in recently characterized enteroendocrine precursor cells that co-express *Bmi1* and *Prox1* [25]. *Prox1*, mammalian ortholog of the *Drosophila* intestinal enteroendocrine transcription factor *Pros*, is expressed by lymphatic endothelial cells as well as by a subset of neuroendocrine cells and their progenitors in the healthy mammalian intestinal epithelium [42]. While *Prox1*-positive cells as a whole do not appear to display a stem cell phenotype in the normal intestine (Wiener, Cell Rep 2014), the subset of these cells that also co-expresses *Bmi1* but not *Lgr5* was shown to have stem cell activity under both homeostatic conditions and after injury [25]. Results from our study now indicate that progastrin expression is a feature of these *Prox1*+/*Bmi1*+/*Lgr5*-low cells in the

healthy intestine. Accordingly, we found that *Gast* expression was concentrated in *Bmi1*+ cells rather than other cell subsets in mice carrying a *Bmi1*-GFP intestinal knock-in [23]. *Bmi1*+ cells and *Bmi1*+/*Prox1*+ cells appear able to replace *Lgr5*- high intestinal stem cells when these are ablated, for example after irradiation, and our current results indicate that progastrin expression decreases, at least transiently, during the original transition from *Bmi1*^{GFP} to *Lgr5*- high cells following whole-body irradiation in mice. In contrast, we show that progastrin expression becomes a feature of *Lgr5*- high cells from the early stage of colonic neoplasia, similar to the emerging co-expression between *Prox1* and *Lgr5* in developing colorectal tumors [43]. Considering the previously reported role for increased endogenous [33] and experimentally-induced progastrin production [13,15] in the resistance of colorectal tumors to radiation damage, and since us and others have shown that progastrin promotes the maintenance and expansion of stem/cancer stem cells in the colon [40], this data suggests that progastrin expression may contribute to the radio-resistance of LGR5- high cells in colorectal tumors.

Our data also indicate that progastrin is produced by colonic cells located towards the lower third of colonic crypts in close proximity to epithelial progenitor cells, which were recently characterized as expressing GPR56, a receptor for this peptide [40]. This result is in accordance with a local physiological role for progastrin in the maintenance of colonic epithelium size and proliferation. Indeed, the proliferation of colonic epithelial cells is increased in progastrin-overexpressing mice [44] but reduced in mice expressing a knockout of the *GAST* gene, which encodes progastrin [18]. In addition, genetic inactivation of the Gpr56-encoding *Adgrg1* gene in mice was shown to inhibit progastrin-driven proliferation and to increase apoptosis in the colonic epithelium [40], suggesting that this receptor may be a key mediator of progastrin activity within specific cell types in this tissue. Thus, when analyzing the single cell RNAseq data extracted from [25], we detected robust Gpr56 expression within Lgr5- high and Bmi1+ cells (including some of the Bmi1+/Prox1+ cells) as well as within a small proportion of Lgr5-low cells, whereas the other putative progastrin receptors Cck2r [19] and Annexin II [39] were respectively not detected or ubiquitously expressed across all cell populations.

In addition, our results suggest that, while human and murine intestinal Lgr5- high cells respectively produce low to negligible amounts of progastrin under physiological conditions, they do so in early pre-neoplastic lesions such as human and mice adenomas. This suggests that progastrin production in preneoplastic Lgr5- high cells may be a *de novo* event, most likely emerging as a consequence of increasing Wnt signaling. Indeed, the *Gast* gene has previously been characterized as a Wnt target gene before [4]. However, the presence of detectable progastrin production in Lgr5-low, Bmi1+/Prox1+ enteroendocrine precursors in the healthy intestinal mucosa, along with the demonstrated ability of these cells to convert to a Lgr5- high phenotype during crypt regeneration [23,25], raises the intriguing alternative possibility that Lgr5- high cells could emerge from Bmi1+/Prox1+ cells during neoplastic transformation of adenomas. Indeed, Prox1 was shown to specifically localize in dysplastic colonic adenomas rather than hyperplastic crypts, and to play an active role in promoting dysplasia [42]. Accordingly, progastrin production is particularly elevated in hyperplastic polyps undergoing dysplasia [11], and our present results demonstrate that progastrin expression is greatly enriched in Lgr5- high cells in mouse and human adenomas. Thus the transition of Progastrin expression from Bmi1+/Prox1+ to Lgr5- high cells may underlie the role of this peptide in sustaining mitotic activity in the mouse colonic after radiation-induced DNA damage [13], a situation where conversion of Bmi1+/Prox1+ cells into Lgr5-high stem cells contributes to the regenerative process [23,25].

Finally, the expression of progastrin by Lgr5- high cells from early stages of tumorigenesis is in accordance with its demonstrated tumor-promoting role in mouse and human intestinal neoplasia. *Gast*-deficiency was demonstrated to decrease the number of intestinal polyps and to reduce polyp proliferation in *Apc*(min-/+) mice [4] and we showed that targeting progastrin via *in vivo* siRNA injection recapitulated this effect and decreased Wnt pathway activation in another model of *Apc* mutation-induced intestinal neoplasia [2], demonstrating the feed-forward mechanisms involving progastrin as both a target and a promoter of Wnt signaling. Our current study indicates that this process emerges from the very first step of the tumorigenic process in the mouse intestine and suggests that this is also the case in human colonic adenomas.

Declaration of Competing Interest

None of the authors has a conflict of interest

Credit authorship contribution statement

Julie Giraud: Conceptualization, Methodology, Format analysis, Writing - Review & Editing and Visualization. **M. Foroutan:** Data Curation, Methodology and Format analysis. **J. Boubaker-Vitre:** Method-

ology, Format analysis and Visualization. **F. Grillet:** Methodology and Format analysis. **U. Jadhav:** Methodology and Investigation. **P. Crespy:** Methodology and Investigation. **C. Breuker:** Methodology and Investigation. **J-F. Bourgaux:** Ressources. **J. Hazerbroucq:** Ressources. **C. Pignodel:** Ressources. **B. Brulin :** Methodology. **R.A. Shivdasani :** Ressources and Writing - Review & Editing. **P. Jay:** Methodology and Writing - Review & Editing. **F. Hollande:** Conceptualization, Writing - Original Draft, Writing - Review & Editing, Visualization, Project administration, Supervision and Funding acquisition. **J. Pannequin:** Conceptualization, Writing - Original Draft, Writing - Review & Editing, Visualization, Project administration, Supervision and Funding acquisition.

Acknowledgments

Authors warmly acknowledge Muriel Asari for her help in the figure construction

Fundings

FH was supported by research grants from the Australian NH&MRC (GNT1164081) and the Tour de Cure Foundation.

JP was supported by the “region Languedoc Roussillon” and by SIRIC Montpellier Cancer Grant INCa_Inserm_DGOS_12553.

JG received a scholarship from “Foundation pour la Recherche Médicale”, and FG a scholarship from the “Ligue nationale contre le cancer”

Supplementary materials

Supplementary material associated with this article can be found, in the online version, at doi:10.1016/j.tranon.2020.101001.

References

- [1] S. Cobb, T. Wood, J. Ceci, A. Varro, M. Velasco, P. Singh, Intestinal expression of mutant and wild-type progastrin significantly increases colon carcinogenesis in response to azoxymethane in transgenic mice, *Cancer* 100 (2004) 1311–1323.
- [2] J. Pannequin, N. Delaunay, M. Buchert, F. Surrel, J.-F. Bourgaux, J. Ryan, S. Boireau, J. Coelho, A. Pélégryn, P. Singh, et al., Beta-catenin/Tcf-4 inhibition after progastrin targeting reduces growth and drives differentiation of intestinal tumors, *Gastroenterology* 133 (2007) 1554–1568.
- [3] P. Singh, A. Owlia, A. Varro, B. Dai, S. Rajaraman, T. Wood, Gastrin gene expression is required for the proliferation and tumorigenicity of human colon cancer cells, *Cancer Res.* 56 (1996) 4111–4115.
- [4] T.J. Koh, C.J. Bulitta, J.V. Fleming, G.J. Dockray, A. Varro, T.C. Wang, Gastrin is a target of the beta-catenin/TCF-4 growth-signaling pathway in a model of intestinal polyposis, *J. Clin. Invest.* 106 (2000) 533–539.
- [5] P.J. Morin, A.B. Sparks, V. Korinek, N. Barker, H. Clevers, B. Vogelstein, K.W. Kinzler, Activation of beta-catenin-Tcf signaling in colon cancer by mutations in beta-catenin or APC, *Science* 275 (1997) 1787–1790.
- [6] J.L. Bos, E.R. Fearon, S.R. Hamilton, M. Verlaan-de Vries, J.H. van Boom, A.J. van der Eb, B. Vogelstein, Prevalence of ras gene mutations in human colorectal cancers, *Nature* 327 (1987) 293–297.
- [7] M.L. Kochman, J. DelValle, C.J. Dickinson, C.R. Boland, Post-translational processing of gastrin in neoplastic human colonic tissues, *Biochem. Biophys. Res. Commun.* 189 (1992) 1165–1169.
- [8] J. Nemeth, B. Taylor, S. Pauwels, A. Varro, G.J. Dockray, Identification of progastrin derived peptides in colorectal carcinoma extracts, *Gut* 34 (1993) 90–95.
- [9] W.W. Van Solinge, F.C. Nielsen, L. Friis-Hansen, U.G. Falkmer, J.F. Rehfeld, Expression but incomplete maturation of progastrin in colorectal carcinomas, *Gastroenterology* 104 (1993) 1099–1107.
- [10] A.M. Smith, S.A. Watson, Gastrin and gastrin receptor activation: an early event in the adenoma-carcinoma sequence, *Gut* 47 (2000) 820–824.
- [11] C. Do, C. Bertrand, J. Palasse, M.-B. Delisle, A. Shulkes, E. Cohen-Jonathan-Moyal, A. Ferrand, C. Seva, A new biomarker that predicts colonic neoplasia outcome in patients with hyperplastic colonic polyps, *Cancer Prev. Res. Phila. Pa* 5 (2012) 675–684.
- [12] F. Wang, J. Flanagan, N. Su, L.-C. Wang, S. Bui, A. Nielson, X. Wu, H.-T. Vo, X.-J. Ma, Y. Luo, RNAscope: a novel *in situ* RNA analysis platform for formalin-fixed, paraffin-embedded tissues, *J. Mol. Diagn. JMD* 14 (2012) 22–29.
- [13] P.D. Ottewill, A.J.M. Watson, T.C. Wang, A. Varro, G.J. Dockray, D.M. Pritchard, Progastrin stimulates murine colonic epithelial mitosis after DNA damage, *Gastroenterology* 124 (2003) 1348–1357.
- [14] P.D. Ottewill, A. Varro, G.J. Dockray, C.M. Kirton, A.J.M. Watson, T.C. Wang, R. Dimalline, D.M. Pritchard, COOH-terminal 26-amino acid residues of progastrin are sufficient for stimulation of mitosis in murine colonic epithelium *in vivo*, *Am. J. Physiol. Gastrointest. Liver Physiol.* 288 (2005) G541–G549.

- [15] A. Prieur, M. Cappellini, G. Habif, M.-P. Lefranc, T. Mazard, E. Morency, J.-M. Pascussi, M. Flacelière, N. Cahuzac, B. Vire, et al., Targeting the Wnt pathway and cancer stem cells with anti-progastrin humanized antibodies as a potential treatment for K-RAS-mutated colorectal cancer, *Clin. Cancer Res. Off. J. Am. Assoc. Cancer Res.* 23 (2017) 5267–5280.
- [16] P. Singh, M. Velasco, R. Given, M. Wargovich, A. Varro, T.C. Wang, Mice overexpressing progastrin are predisposed for developing aberrant colonic crypt foci in response to AOM, *Am. J. Physiol. Gastrointest. Liver Physiol.* 278 (2000) G390–G399.
- [17] P. Singh, M. Velasco, R. Given, A. Varro, T.C. Wang, Progastrin expression predisposes mice to colon carcinomas and adenomas in response to a chemical carcinogen, *Gastroenterology* 119 (2000) 162–171.
- [18] T.J. Koh, J.R. Goldenring, S. Ito, H. Mashimo, A.S. Kopin, A. Varro, G.J. Dockray, T.C. Wang, Gastrin deficiency results in altered gastric differentiation and decreased colonic proliferation in mice, *Gastroenterology* 113 (1997) 1015–1025.
- [19] G. Jin, V. Ramanathan, M. Quante, G.H. Baik, X. Yang, S.S.W. Wang, S. Tu, S.A.K. Gordon, D.M. Pritchard, A. Varro, et al., Inactivating cholecystokinin-2 receptor inhibits progastrin-dependent colonic crypt fission, proliferation, and colorectal cancer in mice, *J. Clin. Investig.* 119 (2009) 2691–2701.
- [20] J. Giraud, L.M. Failla, J.-M. Pascussi, E.L. Lagerqvist, J. Ollier, P. Finetti, F. Bertucci, C. Ya, I. Gasmí, J.-F. Bourgaux, et al., Autocrine secretion of progastrin promotes the survival and self-renewal of colon cancer stem-like cells, *Cancer Res.* 76 (2016) 3618–3628.
- [21] S. Colnot, T. Decaens, M. Niwa-Kawakita, C. Godard, G. Hamard, A. Kahn, M. Giovannini, C. Perret, Liver-targeted disruption of Apc in mice activates beta-catenin signaling and leads to hepatocellular carcinomas, *Proc. Natl. Acad. Sci. USA* 101 (2004) 17216–17221.
- [22] N. Barker, J.H. van Es, J. Kuipers, P. Kujala, M. van den Born, M. Cozijnsen, A. Haegebarth, J. Korving, H. Begthel, P.J. Peters, et al., Identification of stem cells in small intestine and colon by marker gene Lgr5, *Nature* 449 (2007) 1003–1007.
- [23] U. Jadhav, M. Saxena, N.K. O'Neill, A. Saadatpour, G.-C. Yuan, Z. Herbert, K. Murata, R.A. Shivdasani, Dynamic reorganization of chromatin accessibility signatures during dedifferentiation of secretory precursors into Lgr5+ intestinal stem cells, *Cell Stem Cell* 21 (2017) 65–77.
- [24] M.D. Robinson, D.J. McCarthy, G.K. Smyth, edgeR: a Bioconductor package for differential expression analysis of digital gene expression data, *Bioinforma. Oxf. Engl.* 26 (2010) 139–140.
- [25] K.S. Yan, O. Gevaert, G.X.Y. Zheng, B. Anchang, C.S. Probert, K.A. Larkin, P.S. Davies, Z.-F. Cheng, J.S. Kaddis, A. Han, et al., Intestinal enteroendocrine lineage cells possess homeostatic and injury-inducible stem cell activity, *Cell Stem Cell* 21 (2017) 78–90 e6.
- [26] A.T.L. Lun, J.C. Marioni, Overcoming confounding plate effects in differential expression analyses of single-cell RNA-seq data, *Biostat. Oxf. Engl.* 18 (2017) 451–464.
- [27] A. Butler, P. Hoffman, P. Smibert, E. Papalexi, R. Satija, Integrating single-cell transcriptomic data across different conditions, technologies, and species, *Nat. Biotechnol.* 36 (2018) 411–420.
- [28] E.Z. Macosko, A. Basu, R. Satija, J. Nemes, K. Shekhar, M. Goldman, I. Tirosh, A.R. Bialas, N. Kamitaki, E.M. Martersteck, et al., Highly parallel genome-wide expression profiling of individual cells using nanoliter droplets, *Cell* 161 (2015) 1202–1214.
- [29] R. Satija, J.A. Farrell, D. Gennert, A.F. Schier, A. Regev, Spatial reconstruction of single-cell gene expression data, *Nat. Biotechnol.* 33 (2015) 495–502.
- [30] L. Scrucca, M. Fop, T.B. Murphy, A.E. Raftery, mclust 5: clustering, classification and density estimation using Gaussian finite mixture models, *R J.* 8 (2016) 289–317.
- [31] C.M. Royston, J. Polak, S.R. Bloom, W.M. Cooke, R.C. Russell, A.G. Pearce, J. Spencer, R.B. Welbourn, J.H. Baron, G cell population of the gastric antrum, plasma gastrin, and gastric acid secretion in patients with and without duodenal ulcer, *Gut* 19 (1978) 689–698.
- [32] G.G. Finley, R.A. Koski, M.F. Melhem, J.M. Pipas, A.I. Meisler, Expression of the gastrin gene in the normal human colon and colorectal adenocarcinoma, *Cancer Res.* 53 (1993) 2919–2926.
- [33] A. Kowalski-Chauvel, V. Gouaze-Andersson, A. Vignolle-Vidoni, C. Delmas, C. Toulas, E. Cohen-Jonathan-Moyal, C. Seva, Targeting progastrin enhances radiosensitization of colorectal cancer cells, *Oncotarget* 8 (2017) 58587–58600.
- [34] C.S. Potten, Extreme sensitivity of some intestinal crypt cells to X and gamma irradiation, *Nature* 269 (1977) 518–521.
- [35] J. Muñoz, D.E. Stange, A.G. Schepers, M. van de Wetering, B.-K. Koo, S. Itzkovitz, R. Volckmann, K.S. Kung, J. Koster, S. Radulescu, et al., The Lgr5 intestinal stem cell signature: robust expression of proposed quiescent “+4” cell markers, *EMBO J.* 31 (2012) 3079–3091.
- [36] E. Sangiorgi, M.R. Capecchi, Bmi1 is expressed in vivo in intestinal stem cells, *Nat. Genet.* 40 (2008) 915–920.
- [37] A. Ayyaz, S. Kumar, B. Sangiorgi, B. Ghoshal, J. Gosio, S. Ouladan, M. Fink, S. Barutcu, D. Trcka, J. Shen, et al., Single-cell transcriptomes of the regenerating intestine reveal a revival stem cell, *Nature* 569 (2019) 121–125.
- [38] A.L. Haber, M. Biton, N. Rogel, R.H. Herbst, K. Shekhar, C. Smillie, G. Burgin, T.M. Delorey, M.R. Howitt, Y. Katz, et al., A single-cell survey of the small intestinal epithelium, *Nature* 551 (2017) 333–339.
- [39] P. Singh, H. Wu, C. Clark, A. Owlia, Annexin II binds progastrin and gastrin-like peptides, and mediates growth factor effects of autocrine and exogenous gastrins on colon cancer and intestinal epithelial cells, *Oncogene* 26 (2007) 425–440.
- [40] G. Jin, K. Sakitani, H. Wang, Y. Jin, A. Dubeykovskiy, D.L. Worthley, Y. Taylor, T.C. Wang, The G-protein coupled receptor 56, expressed in colonic stem and cancer cells, binds progastrin to promote proliferation and carcinogenesis, *Oncotarget* 8 (2017) 40606–40619.
- [41] A.-M. Baker, T.A. Graham, G. Elia, N.A. Wright, M. Rodriguez-Justo, Characterization of LGR5 stem cells in colorectal adenomas and carcinomas, *Sci. Rep.* 5 (2015) 8654.
- [42] T.V. Petrova, A. Nykänen, C. Norrmén, K.I. Ivanov, L.C. Andersson, C. Haglund, P. Puolakkainen, F. Wempe, H. von Melchner, G. Gradwohl, et al., Transcription factor PROX1 induces colon cancer progression by promoting the transition from benign to highly dysplastic phenotype, *Cancer Cell* 13 (2008) 407–419.
- [43] S. Ragusa, J. Cheng, K.I. Ivanov, N. Zangger, F. Ceteci, J. Bernier-Latmani, S. Milatos, J.-M. Joseph, S. Tercier, H. Bouzourene, et al., PROX1 promotes metabolic adaptation and fuels outgrowth of Wnt(high) metastatic colon cancer cells, *Cell Rep.* 8 (2014) 1957–1973.
- [44] T.C. Wang, T.J. Koh, A. Varro, R.J. Cahill, C.A. Dangler, J.G. Fox, G.J. Dockray, Processing and proliferative effects of human progastrin in transgenic mice, *J. Clin. Investig.* 98 (1996) 1918–1929.